J. Chem. Sci. (2020)132:12
https://doi.org/10.1007/s12039-019-1702-x

REGULAR ARTICLE

Graphene oxide: an efficient carbocatalyst for the solvent-free synthesis of 2-(substituted benzoyl)-3-(substituted phenyl)imidazo[1,2-*a*]pyridines

DILPREET KOUR[a,b], SONAKSHI SASAN[a] and KAMAL K KAPOOR[a,*]
[a]Department of Chemistry, University of Jammu, Jammu 180 006, India
[b]Department of Chemistry, University Institute of Engineering and Technology, Kathua, University of Jammu, Jammu 184 103, India
E-mail: kamalkka@gmail.com

MS received 28 May 2019; revised 13 August 2019; accepted 15 August 2019

Abstract. GO has been found as a remarkable heterogeneous carbocatalyst for the solvent-free synthesis of 2-(substituted benzoyl)-3-(substituted phenyl)imidazo[1,2-*a*]pyridines from chalcones and 2-aminopyridine. The present methodology offers a novel and eco-friendly approach with appreciable yields of the desired products.

Keywords. 2-(Substituted benzoyl)-3-(substituted phenyl)imidazo[1,2-*a*]pyridines; GO; carbocatalyst; solvent free; recyclability.

1. Introduction

Imidazo[1,2-*a*]pyridines possess a variety of biological activities[1] such as antiulcer,[2] antibacterial,[3] antipyretic,[4] antiviral,[5] anti-inflammatory,[6] andanticancer.[7] This nucleus has gained importance due to its contribution in the area of material science, optoelectronics[8] and organometallics.[9] The therapeutic potential of this nucleus makes it serve as an integral core of various commercially available drugs as shown in (Figure 1).[10] The diversification of applications of this framework generates immense interest among organic chemists to devise newer better protocols for its synthesis.

Since this nucleus is associated with a wide range of biological activities,[1] various analogues of imidazopyridine have been synthesized.[11] One of them is (substituted benzoyl)imidazo[1,2-*a*]pyridine in which substituted benzoyl functionality has been held accountable for its eminent biological properties.[12] With the advances in green and sustainable chemistry, the development of solvent-free methodologies using heterogeneous catalysts has been gaining prime interest.[13] In this regard, Graphene oxide (GO) has evolved as an efficient organic material appreciated as being eco-friendly and versatile carbocatalyst[14] due to its remarkable features like stability, biocompatibility, large surface area and promising electronic, optical, thermal and mechanical properties.[15] The surface of graphene oxide is functionalized with several oxygen-containing groups like carboxyl, epoxy and hydroxyl groups. These functionalities are responsible for the oxidising properities[16] and the acidic nature (pH 4.5 at 0.1 mg mL^{-1})[17] of GO (Figure 2). Owing to their excellent merits of low toxicity and recyclability, Go has played a significant role in carrying out wide range of synthetic organic transformations.[18]

Recently, an iodine mediated preparation of imidazo[1,2-*a*]pyridines[19] has been established in our laboratory. In our quest towards the development of an eco-benign protocol for the preparation of imidazo[1,2-*a*]pyridines and various heterocycles,[20] we wished to employ GO as a heterogeneous carbocatalyst under solvent-free conditions.

*For correspondence

Electronic supplementary material: The online version of this article (https://doi.org/10.1007/s12039-019-1702-x) contains supplementary material, which is available to authorized users.

Published online: 19 December 2019

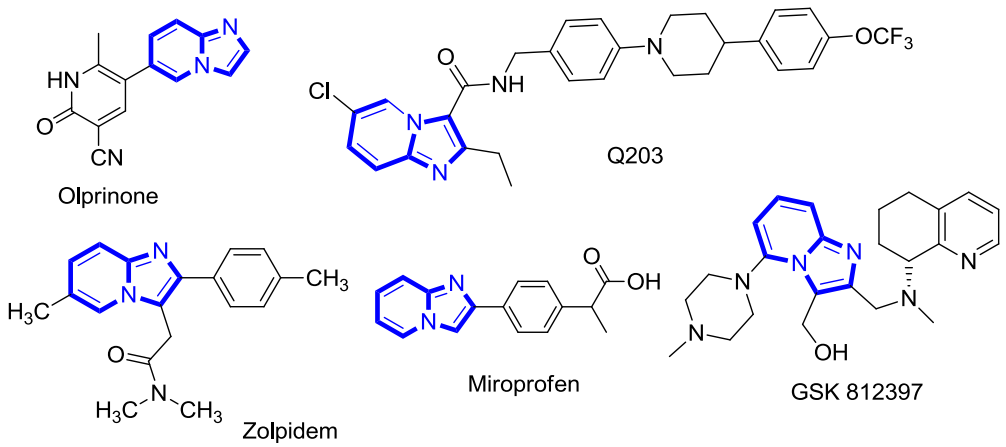

Figure 1. Drugs possessing imidazo[1,2-*a*]pyridine nucleus.

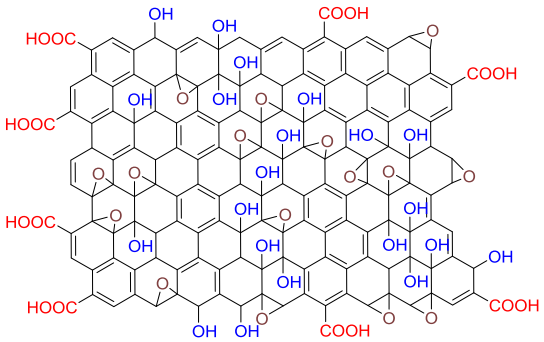

Figure 2. Structural model of Graphene oxide.

2. Experimental

2.1 *General information*

The experiments were performed in an oven-dried glass apparatus and TLC [silica gel pre-coated aluminium sheets (60 F2554, Merck)] analysis was used to monitor the reaction. Column chromatography was performed on silica gel (60–120 mesh). Spots were visualized by UV light, iodine vapours and draggendorff reagent. Solvents were removed using Heidolph rotary vapour. Perfit melting point apparatus was used to measure the melting points. ^{1}H NMR and ^{13}C NMR spectra in $CDCl_3$ as solvents were recorded at respective 400 MHz and 100 MHz on Bruker Avance III-400 MHz spectrometer with tetramethylsilane as an internal reference. The chemical shifts (δ) are expressed in ppm downfield from tetramethylsilane. For the HRMS measurement, Q-TOF was used.

2.2 *General procedure for the synthesis of Graphene oxide (GO)*

The synthesis of GO was realized by improved Hummer's method.[15,21]

In this method, Graphite flakes (1.0 g) were mixed with 9:1 mixture of concentrated H_2SO_4:H_3PO_4 (36:4 mL). The reaction mixture was stirred for half an hour. Then KMnO4 (6 g) was added in the reaction mixture at regular intervals under ice-bath so as to maintain temperature below 4 °C in order to control the exothermic reaction. The reaction mixture was left on stirring for 12 h to allow complete oxidation of graphite. Then the mixture was poured into ice-cold water containing 30% H_2O_2 (3 mL) so as to stop the oxidation process. The suspension was centrifuged and the supernatant was discarded. The solid material was then washed in succession with distilled water, dil. HCl, and ethanol to obtain Graphite oxide which was sonicated for 2 h in distilled water. The solution was then filtered and the solid graphene oxide was then air-dried.

The synthesized GO was in full agreement with the literature report[22] characterised through I.R (Figure 3), SEM (Scanning Electron Microscopy, Figure 4) and XRPD (X-ray Powder Diffraction Pattern, Figure 5) studies.

The nature of functional groups present in GO was also carried out through FT-IR spectral studies. Figure 3 shows $\nu_{(OH)}$ broad band at 3500.95 cm^{-1}, $\nu_{(C=O)}$ band at 1735.93 cm^{-1} and $\nu_{(epoxy)}$ band at 1230.58 cm^{-1}. A sharp band at 1620.21 cm^{-1} is due to bending vibrations of OH group. Presence of carboxylic acid and carbonyl groups at the edges of graphene oxide is indicated due to the presence of absorption band at 742.05 cm^{-1} $\delta_{(C=O)}$ (bending vibrations).

The SEM images of GO clearly shows that it has sheets like morphology and GO sheets are entangled.

The XRPD pattern of GO shows a sharp peak at (2θ) at 10.49° which is the characteristic peak of GO indicating the oxidation of graphite to graphene oxide.

2.3 *General procedure for the synthesis2-(substituted benzoyl)-3-(substituted phenyl)imidazo[1,2-a]pyridines (3a-j)*

In a 25 mL round-bottomed flask, chalcone (0.208 g, 1.0 mmol), 2-aminopyridine (0.112 g, 1.2 mmol), and

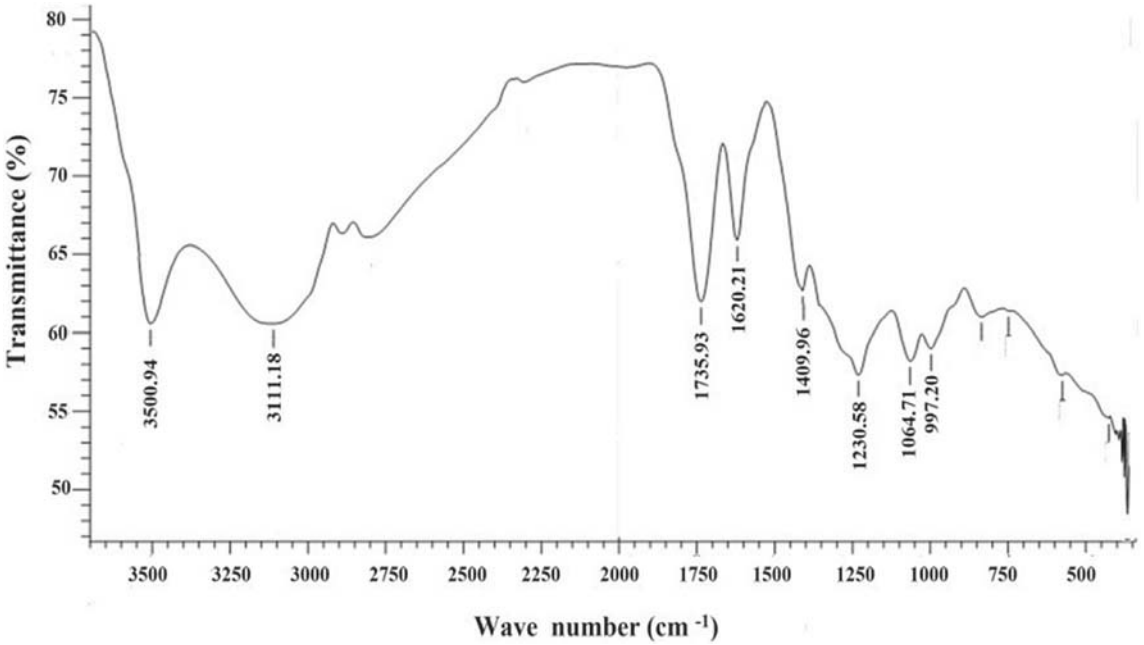

Figure 3. I.R spectrum of GO.

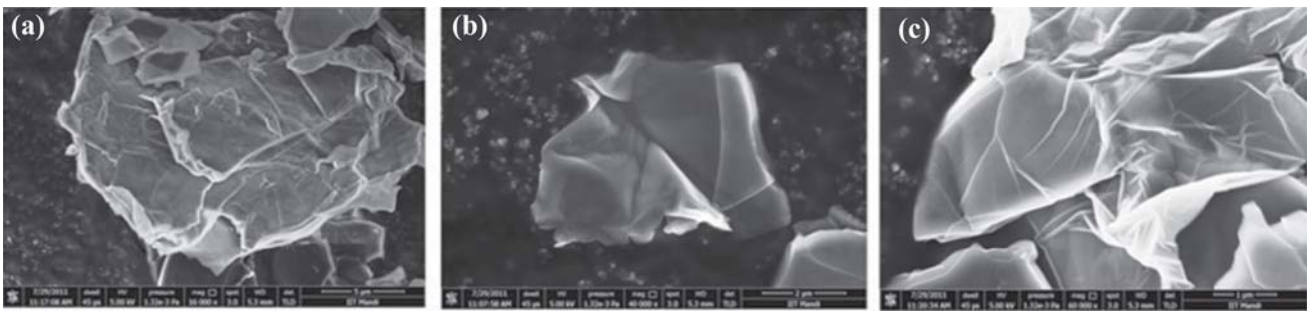

Figure 4. SEM images of GO (a) 16 kx (b) 40 kx (c) 60 kx.

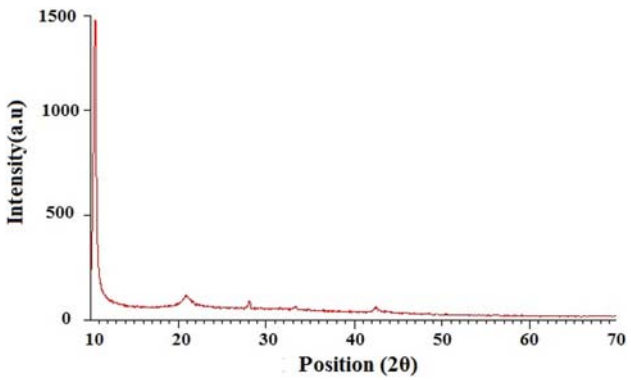

Figure 5. XRPD pattern of GO.

graphene oxide (20 wt % w.r.t chalcone) were taken and the contents were then placed in an oil bath preheated at 120 °C. The reaction was continued till completion (TLC) and then it was allowed to cool to room temperature. Ethanol was added to the reaction mixture followed by the filtration of the catalyst. The filtrate was concentrated and the resulting crude residue was purified by column chromatography to obtain the desired products (**3a-j**) in 76–87% yield.

2.4 *Spectral analysis of the synthesized compounds (3a-j)*

Phenyl(3-phenylimidazo[1,2-*a*]pyridin-2-yl)methanone (3a): ^{1}H NMR (400 MHz, $CDCl_3$): δ 8.21 (d, J = 7.9 Hz, 2H), 8.06 (d, J = 6.9 Hz, 1H), 7.76 (d, J = 9.2 Hz, 1H), 7.62–7.42 (m, 8H), 7.35–7.28 (m, 1H), 6.89 (t, J = 6.8 Hz, 1H).

^{13}C NMR (100 MHz, $CDCl_3$): 190.0, 144.0, 140.2, 137.6, 135.3, 132.7, 131.7, 130.8, 129.3, 128.1, 127.7, 126.7, 126.1, 123.8, 119.2, 114.0. HRMS (ESI) m/z $(M+H)^+$ calcd. for $C_{20}H_{15}N_2O$ 299.1176, found: 299.1181.

Phenyl(3-(*p*-tolyl)imidazo[1,2-*a*]pyridin-2-yl) methanone (3b): ^{1}H NMR (400 MHz, $CDCl_3$): δ 8.12–8.09 (m, 3H), 7.76 (d, J = 9.2 Hz, 1H), 7.58–7.48 (m, 5H), 7.33–7.25 (m, 3H), 6.86 (t, J = 6.8 Hz, 1H), 2.42 (s, 3H).

^{13}C NMR (100 MHz, $CDCl_3$): δ 189.9, 144.4, 143.8, 143.7, 143.3, 140.3, 136.1, 135.6, 135.2, 134.9,130.9, 130.4, 130.3, 129.3, 129.1, 128.8, 128.6, 128.4, 126.0, 124.0, 122.0, 119.0, 113.7, 21.7.

HRMS (ESI) m/z $(M+H)^+$ calcd for $C_{21}H_{17}N_2O$ 313.1333, found: 313.1339.

(*p*-Methoxyphenyl)(3-(*p*-tolyl)imidazo[1,2-*a*]pyridin-2-yl)methanone (3c): ^{1}H NMR (400 MHz, $CDCl_3$): δ 8.25 (d, J = 8.6 Hz, 2H), 8.11 (d, J = 6.9 Hz, 1H), 7.74 (d, J = 9.1 Hz, 1H), 7.45 (d, J = 7.8 Hz, 2H), 7.34–7.26 (m, 3H), 6.95 (d, J = 8.6 Hz, 2H), 6.84 (t, J = 6.8 Hz, 1H), 3.88 (s, 3H), 2.44 (s, 3H).

^{13}C NMR (100 MHz, $CDCl_3$,): δ 188.7, 163.2, 143.6, 140.3, 139.1, 133.2, 132.0, 130.7, 130.2, 129.7, 128.7, 125.7, 125.3, 124.0, 118.9, 113.3, 55.4, 21.4.

HRMS (ESI) m/z $(M+H)^+$ calcd for $C_{22}H_{19}N_2O_2$ 343.1438, found: 343.1433.

(*p*-Methoxyphenyl)(3-(*p*-nitrophenyl)imidazo[1,2-*a*]pyridine-2-yl)methanone (3d): ^{1}H NMR (400 MHz, $CDCl_3$): δ 8.45–8.38 (m, 2H), 8.34–8.28 (m, 2H), 8.11 (d, J = 7.0 Hz, 1H), 7.84–7.77 (m, 3H), 7.42–7.36 (m, 1H), 7.02–6.94 (m, 3H), 3.91(s, 3H).

^{13}C NMR (100 MHz, $CDCl_3$): δ 187.8, 163.9, 141.3, 140.6, 133.3, 131.3, 130.9, 130.2, 128.8, 125.7, 124.2, 123.7, 119.4, 114.4, 114.0, 113.6, 55.4

HRMS (ESI) m/z $(M+H)^+$ calcd for $C_{21}H_{16}N_3O_4$ 374.1133, found: 374.1141.

(3-(*m*-nitrophenyl)imidazo[1,2-*a*]pyridine-2-yl)(phenyl)methanone (3e): ^{1}H NMR ($CDCl_3$, 400 MHz): δ 8.55 (s, 1H), 8.29–8.27 (m, 1H), 8.09–8.05 (m, 2H), 7.97–7.94 (m, 2H), 7.71–7.55 (m, 6H), 7.29 (s, 1H).

^{13}CNMR ($CDCl_3$, 100 MHz,): δ 189.6, 148.7, 141.6, 137.5, 136.6, 134.3, 133.3, 130.8, 130.0, 128.8, 128.6, 128.2, 126.6, 125.2, 124.6, 124.0, 123.4, 122.3, 119.4, 114.6.

HRMS (ESI) m/z $(M+H)^+$ calcd for $C_{20}H_{13}N_3O_3$ 344.1027, found: 344.1036

(*p*-Bromophenyl)(3-(*o*-nitrophenyl)imidazo[1,2-*a*]pyridine-2-yl)methanone (3f): ^{1}H NMR (400 MHz, $CDCl_3$): δ 8.33 (d, J = 8 Hz, 1H), 8.22 (d, J = 8 Hz, 2H), 7.84–7.74 (m, 4H), 7.64– 7.51 (m, 3H), 7.40–7.36 (m, 1H), 6.92 (t, J = 6.8 Hz, 1H).

^{13}CNMR (100 MHz, $CDCl_3$): δ 188.2, 149.5, 144.3, 139.9, 136.1, 133.6, 132.4, 132.0, 131.4, 130.8, 129.5, 128.0, 126.4, 125.2, 125.0, 124.0, 119.3, 114.3. HRMS (ESI) m/z $(M+H)^+$ calcd for $C_{20}H_{13}BrN_3O_3$: 422.0132, found: 422.0143.

Thiophen-2-yl(3-(thiophen-2-yl)imidazo[1,2-*a*]pyridin-2-yl)methanone (3g): ^{1}H NMR (400 MHz, $CDCl_3$): δ 8.48 (d, J = 4 Hz 1H), 8.19 (d, J = 4 Hz, 1H), 7.74–7.69 (m, 2H), 7.57 (d J = 4 Hz, 1H), 7.41 (d, J = 4 Hz, 1H), 7.32–7.28 (m, 1H), 7.21–7.17 (m, 2H), 6.87 (t, J = 6.8 Hz, 1H).

^{13}C NMR (100 MHz, $CDCl_3$): δ 180.6, 144.2, 143.4, 140.8, 136.1, 134.7, 130.4, 128.6, 127.9, 127.4, 126.5, 124.5, 121.6, 118.9, 114.0. HRMS (ESI) m/z $(M+H)^+$ calcd for $C_{16}H_{11}N_2OS_2$: 311.0305, found: 311.0305.

Benzo[*d*][1,3]dioxol-4-yl(3-phenylimidazo[1,2-*a*]pyridin-2-yl)methanone (3h): ^{1}H NMR (400 MHz, $CDCl_3$): δ 8.09 (d, J = 7.0 Hz, 1H), 7.91 (d, J = 8.2 Hz, 1H), 7.75–7.71 (m, 2H), 7.56–7.47 (m, 5H), 7.31–7.27 (m, 1H), 6.86–6.82 (m, 2H), 6.02 (s, 2H).

^{13}CNMR (100 MHz, $CDCl_3$): δ 188.2, 151.5, 147.6, 143.7, 140.2, 132.3, 130.3, 130.1, 129.1, 128.9, 128.6, 128.3, 127.7, 125.9, 123.9, 118.9, 113.6, 110.5, 107.7, 101.6.

HRMS (ESI) m/z $(M+H)^+$ calcd for $C_{21}H_{15}N_2O_3$: 343.1074, found 343.1070.

Benzo[*d*][1,3]dioxol-4-yl(8-nitro-3-phenylimidazo[1,2-*a*]pyridin-2-yl)methanone (3i): ^{1}H NMR (400 MHz, $CDCl_3$) δ 9.18 (s, 1H), 8.09–8.06 (m, 1H), 7.92–7.88 (m, 1H), 7.83 (d, J = 9.9 Hz, 1H), 7.69 (s, 1H), 7.62–7.53 (m, 5H), 6.88 (d, J = 8.2 Hz, 1H), 6.07 (s, 2H).

^{13}C NMR (100 MHz, $CDCl_3$): δ 187.0, 152.0, 147.8, 143.4, 143.1, 138.3, 131.6, 130.9, 130.2, 129.4, 127.9, 126.5, 124.5, 119.9, 118.8, 110.2, 107.8, 101.8

HRMS (ESI) m/z $(M+H)^+$ calcd for $C_{21}H_{14}N_3O_5$: 388.0925, found: 388.0930.

(6-Methyl-3-phenylimidazo[1,2-*a*]pyridin-2-yl(*p*-tolyl)-methanone (3j): ^{1}H NMR (400 MHz, $CDCl_3$) δ 8.10 (d, J = 8.1 Hz, 2H), 7.86 (s, 1H), 7.65 (d, J = 9.3 Hz, 1H), 7.58–7.46 (m, 5H), 7.25 (d, J = 8.0 Hz, 2H), 7.15 (d, J = 9.3 Hz, 1H), 2.41 (s, 3H), 2.31 (s, 3H).

^{13}CNMR (100 MHz, $CDCl_3$): δ 189.9, 143.1, 142.9, 140.3, 135.4, 130.8, 130.4, 129.1, 129.0, 128.9, 128.7, 128.6, 128.4, 123.4, 121.2, 118.3, 21.6, 18.4. HRMS (ESI) m/z $(M+H)^+$ calcd for $C_{22}H_{19}N_2O$ 327.1489, found: 327.1496.

3. Results and Discussion

3.1 *Chemistry*

We envisioned our study by reacting chalcones **1a** (1 mmol) and 2-aminopyridine **2a** (1.2 mmol) as a prototype in the presence of 35 wt % GO[21] under solvent-free conditions at 120 °C. To our delight, the completion of reaction was noticed within 20 min with the formation of product **3a** in 87% yield (entry 1, Table 1). Encouraged with the result, the above-mentioned reaction was optimized under different conditions by varying the amount of GO at different temperatures and in different solvents. The results for

Table 1. Optimization of reaction conditions[a]

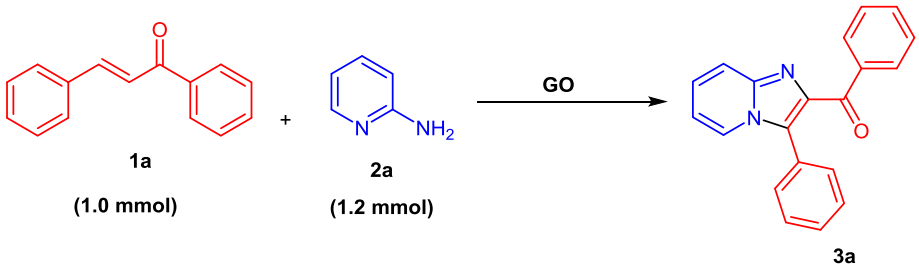

Sl. No.	Catalyst	Solvent	Temp. (°C)	Yield (%)[b]
1	GO (35 wt%)	–	120	87%
2	GO (50 wt%)	–	120	85%
3	**GO (20 wt%)**	–	**120**	**87%**
4	GO (10 wt%)	–	120	72%
5	NIL	–	120	–
6	GO (20 wt%)	–	130	83%
7	GO (20 wt%)	–	100	70%
8	GO (20 wt%)	EtOH	Reflux	74%
9	GO (20 wt%)	Toluene	Reflux	80%
10	GO (20 wt%)	CH_3CN	Reflux	60%
11	GO (20 wt%)	DMF	Reflux	56%
12	GO (20 wt%)	1,4-Dioxane	Reflux	40%

[a]Carried out with chalcone (1.0 mmol), 2-aminopyridine(1.2 mmol), GO (20 wt %), at 120 °C
[b]Isolated yield after column chromatography purification

the optimization of the reaction conditions are summarized in Table 1. No significant enhancement in the yield of the product was observed by increasing the amount of GO (entry 1–3, Table 1), however, yield decreases significantly by using lesser amount of GO (entry 4, Table 1). Subsequent examination of the temperature on the model reaction proved that 120 °C was the optimal requirement of the reaction (entries 3, 6–7, Table 1). Afterwards, screening of various solvents revealed that the best yield of the product **3a** was obtained under solvent-free conditions (entries 3, 8–12, Table 1). It was also noticed that in absence of GO, there was no formation of product **3a** (entry 5, Table 1). Eventually, it is evident from the Table 1 that the best results of the reaction were obtained at 120 °C with 20 wt% of GO under solvent-free conditions (entry 3, Table 1).

The substrate scope of present methodology was investigated by employing variedly substituted chalcones and 2-aminopyridines (Table 2). Chalcones

Table 2. Substrate scope of 2-(substituted benzoyl)-3-(substituted phenyl)imidazo[1,2-*a*]pyridines[a,b]

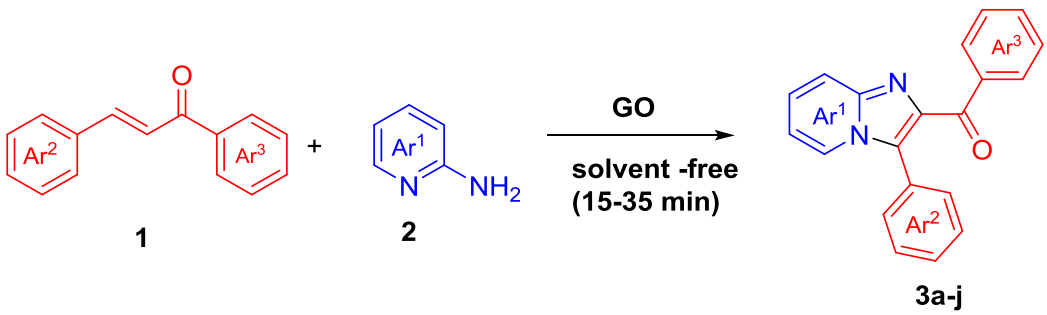

Table 2. (Continued.)

Entry	Substrate	Physical appearance	Time (in min.)	Yield	Melting point
3a	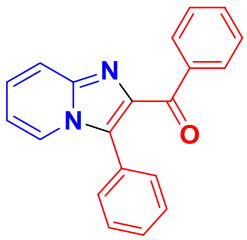	Creamy solid	30	87% (260 mg)	108–110 °C
3b	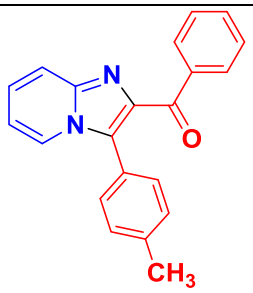	Oil	20	82% (256 mg)	-
3c	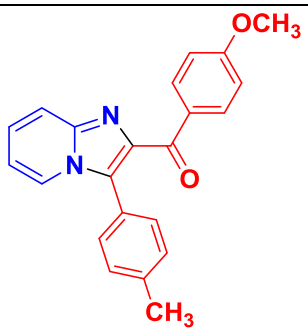	Yellow solid	20	84% (288 mg)	123–125 °C
3d	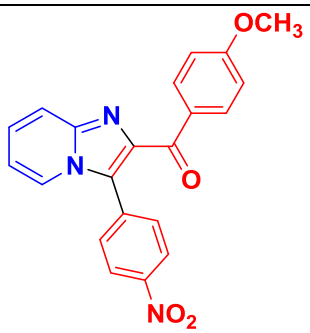	Oil	20	78% (291 mg)	-

Table 2. (Continued.)

Entry	Substrate	Physical appearance	Time (in min.)	Yield	Melting point
3e	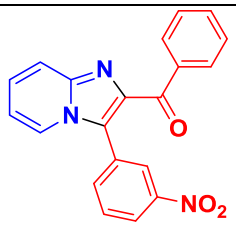	Oil	25	80% (275 mg)	-
3f	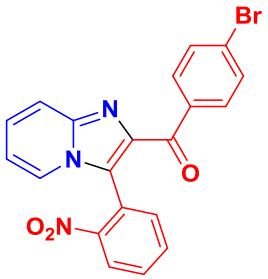	Shiny brown solid	20	85% (358 mg)	136–139 °C
3g	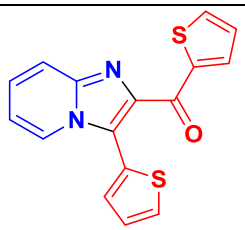	Crystalline yellow solid	20	86% (267 mg)	160–163 °C
3h	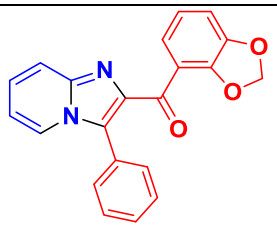	Oil	30	76% (260 mg)	-
3i	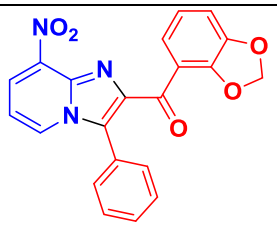	Brown solid	25	82% (318 mg)	216–218 °C
3j	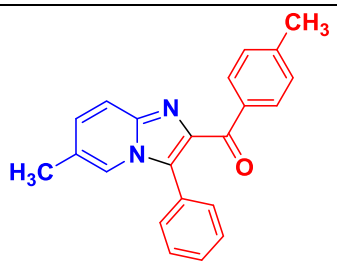	White solid	15	80% (261mg)	156–158 °C

[a]**1** (1 mmol), **2** (1.0 mmol), GO (20 wt%), at 120 °C.
[b]isolated yields after column chromatography.

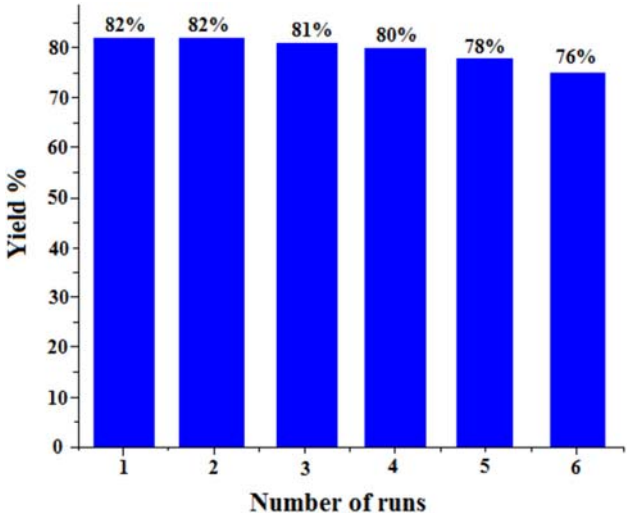

Figure 6. Recyclability of catalyst.

bearing electron-attracting (Cl, Br, NO_2) and electron-donating groups (Me, OMe) were converted to the corresponding2-(substituted benzoyl)-3-(substituted phenyl)imidazo[1,2-*a*]pyridines in appreciable yields. Furthermore, the construction of 2-(substituted benzoyl)-3-(substituted phenyl)imidazo[1,2-*a*]pyridines bearing heteryl ring systems (entries 3g, Table 2) as well as an oxymethylene moiety (entries 3h-i, Table 2) were also achieved under the same reaction conditions.

3.2 *Recyclability of catalyst*

To investigate the recyclability of GO, the residual GO was collected from the reaction and washed with ethanol (3 x 5 mL) to remove all the residual organic substances followed by drying in air. The recovered GO was then reused for the next five consecutive runs for the synthesis of **3a** and results revealed no significant loss of catalytic activity (Figure 6).

The IR spectra of the catalyst recovered after alternate runs were recorded and were compared with the IR spectra of the catalyst before the reaction. The comparative analysis of IR spectra showed no major changes in the characteristics bands (Figure 7).

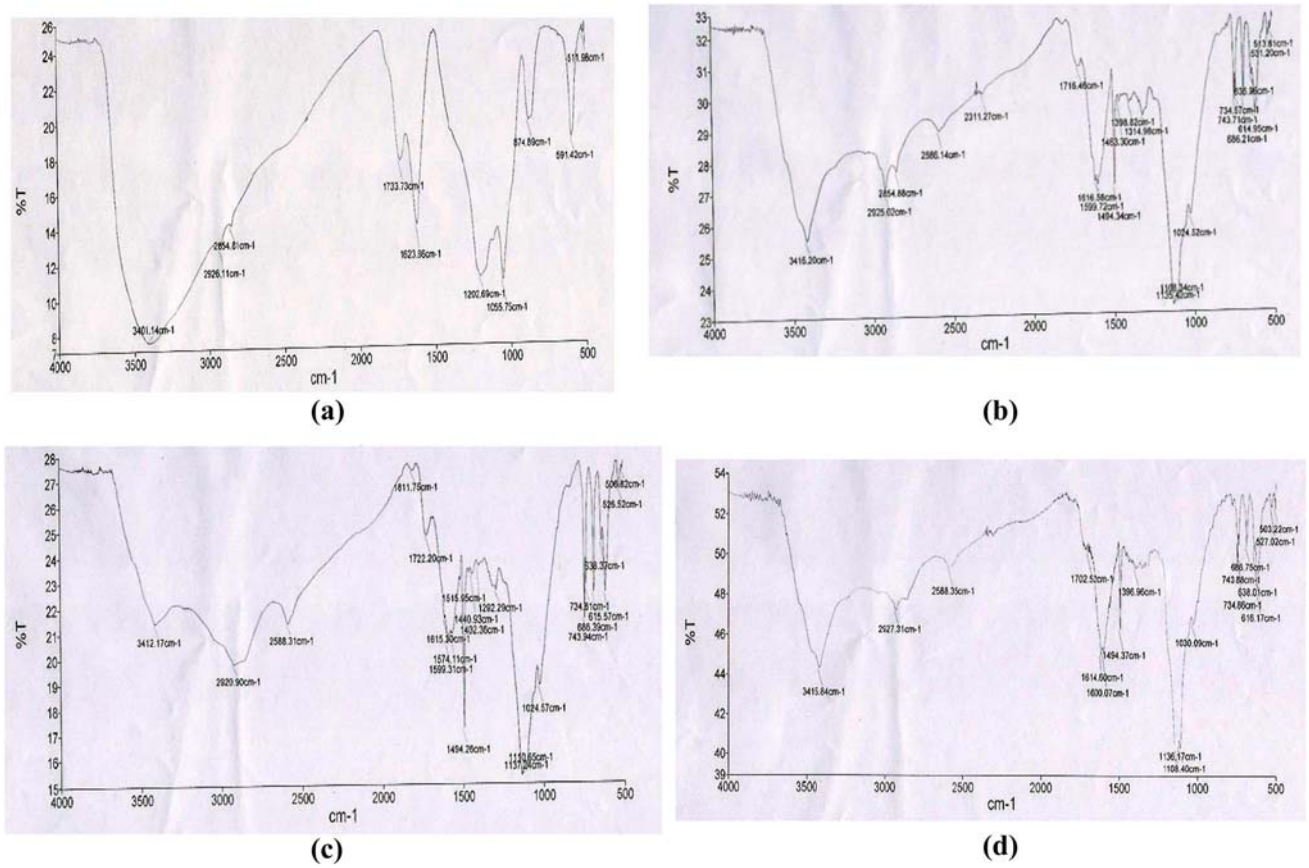

Figure 7. (A) IR spectrum of Graphene oxide before reaction (B) IR spectrum of Graphene oxide after 1st run (C) IR spectrum of Graphene oxide after 3rd run (D) IR spectrum of Graphene oxide after 5th run.

4. Conclusions

We have developed a simple, solvent-free approach for the synthesis of 2-(substituted benzoyl)-3-(substituted phenyl)imidazo[1,2-*a*]pyridines from chalcones and 2-aminopyridines by employing a heterogeneous carbocatalyst GO. This protocol makes the use of readily available precursors and thus offers significant flexibility to access a variety of imidazopyridines with various substitution patterns. The present method is fast, economical, milder and environment-friendly.

Supplementary Information (SI)

Supplementary information for this article is available at www.ias.ac.in/chemsci.

Acknowledgements

The authors are thankful to the Department of Chemistry, University of Jammu for providing all the necessary facilities and Department of Science and Technology, Government of India, New Delhi for NMR facility under PURSE.

References

1. Lhassani M, Chavignon O, Chezal J M, Teulade J C, Chapat J P, Snoec R, Andrei G, Balzarini, J, Clercq E D and Gueiffier A 1999 Synthesis and antiviralactivity of imidazo[1,2-a]pyridines *Eur. J. Med. Chem*. **34** 271
2. Kaminski J J and Doweyko A M 1997 Antiulcer agents. 6. Analysis of the in vitro biochemical and in vivo gastric antisecretory activity of substituted imidazo[1,2-*a*]pyridines and related analogues using comparative molecular field analysis and hypothetical active site lattice methodologies *J. Med. Chem*. **40** 427
3. Byth K F, Culshaw J D, Green S, Oakes S E and Thomas A P 2004 Imidazo[1,2-*a*]pyridines. Part 2: SAR and optimisation of a potent and selective class of cyclin-dependent kinase inhibitors *Bioorg. Med. Chem. Lett*. **14** 2245
4. Almirante L, Polo L, Mugnaini A, Provinciali E, Rugarli P, Biancotti A, Gamba A and Murmann W 1965 Derivatives of imidazole. I. Synthesis and reactions of imidazo[1,2-*a*]pyridines with analgesic, antiinflammatory, antipyretic, and anticonvulsant activity *J. Med. Chem*. **8** 305
5. Elkakmaoui A, Gueiffier A, Milhavet J C, Blache Y, Chapat J P, Chavignon O, Teulade J C, Snoeck R, Andrei G and Clerc E D 1994 Synthesis and antiviral activity of 3-substituted imidazo[1,2-*a*]pyridines *Bioorg. Med. Chem. Lett.* **4** 19
6. Lacerda R B, de Lima C K F, da Silva L L, Romeiro N C, Miranda A L P, Barreiro E J and Fraga C A M 2009 Discovery of novel analgesic and anti-inflammatory 3-arylamine-imidazo[1,2-*a*]pyridine symbiotic prototypes *Bioorg. Med. Chem*. **17** 74
7. Hamdouchi C, Blas J. D, Prado M D, Gruber J, Heinz B A and Vance L 1992 Amino-3-substituted-6-[(E)-1-phenyl-2-(N-methylcarbamoyl)vinyl]imidazo[1,2-*a*]pyridines as a novel class of inhibitors of human rhinovirus: stereospecific synthesis and antiviral activity *J. Med. Chem*. **42** 50
8. (a) Wan J, Zheng C J, Fung M K, Li X K, Lee C S and Zhang X H 2012 Multifunctional electron-transporting indolizinederivatives for highly efficient blue fluorescence, orange phosphorescence host and two-color based white OLEDs *J. Mater. Chem*. **22** 450; (b) Stasyuk A Banasiewicz J M, Cyranski M K and Gryko D T 2012 Imidazo[1,2-*a*]pyridines Susceptible to Excited State Intramolecular Proton Transfer: One-Pot Synthesis via an Ortoleva–King Reaction *J. Org. Chem.* **77** 5552; (c) John A, Shaikh M M and Ghosh P 2009 Palladium complexes of abnormal N-heterocyclic carbenes as precatalysts for the much preferred Cu-free and amine-free Sonogashira coupling in air in a mixed-aqueous medium *Dalton Trans.* 10581
9. (a) Douhal A, Guerri F A and Acuna A U 1995 Photoinduced intramolecular proton transfer and charge redistribution in imidazopyridines *J. Phys. Chem.* **99** 76; (b) Douhal A, Guerri F A and Acuna A U 1997 Probing nanocavities with proton-transfer fluorescence *Angew. Chem. Int. Ed. Engl.* **l36** 1514
10. Pericherla K, Kaswan P, Pandey K and Kumar A 2015 Recent developments in the synthesis of imidazo[1,2-*a*]pyridines *Synthesis* **47** 887
11. (a) Kang S, Kim R Y, Seo M J, Lee S, Kim Y M Seo M, Seo J J, Ko Y, Choi I, Jang J, Nam J, Park S, Kang H Kim H J, Kim J, Ahn S, Pethe K, Nam K, No Z and Kim J 2014 Lead optimization of a novel series of imidazo[1,2-*a*]pyridine amides leading to a clinical candidate (Q203) as a multi- and extensively-drug-resistant anti-tuberculosis agent *J. Med. Chem.* **57** 5293; (b) Masurier N, Debiton E, Jacquemet A, Bussiere A, Chezal J M, Ollivier A, Tetegan D, Andaloussi M, Galmier M J, Lacroix J, Canitrot D, Teulade J C, Gaudreault R C, Chavignon O and Moreau E 2012 Imidazonaphthyridine systems (part 2): Functionalization of the phenyl ring linked to the pyridine pharmacophore and its replacement by a pyridinone ring produces intriguing differences in cytocidal activity *Eur. J. Med. Chem.* **52** 13
12. (a) Kaswan P, Pericherla K, Rajnikant and Kumar A 2014 Synthesis of 3-aroylimidazo[1,2-*a*]pyridines via $CuCl_2$ catalyzed tandem dual carbon–nitrogen bonding *Tetrahedron* **70** 8539; (b) Kaswan P, Pericherla K, Saini H K and Kumar A 2015 One-pot, three component tandem reaction of 2-aminopyridines, acetophenones and aldehydes: synthesis of 3-aroylimidazo[1,2-*a*]pyridines *RSC Adv.* **5** 3670; (c) Meng X, Zhang J, Chen B, Jing Z and Zhao P 2016 Copper supported on H^+-modified manganese oxide octahedral molecular sieves (Cu/H-OMS-2) as a heterogeneous biomimetic catalyst for the synthesis of imidazo[1,2-*a*]-N-heterocycles *Catal. Sci. Technol*. **6** 890; (d) Reddy K R, Reddy A S, Shankar R, Rajnikant and Das P 2015 Copper-catalyzed oxidative C−H amination: Synthesis of imidazo[1,2-*a*]-N-heterocycles from N-heteroaryl enaminones *Asian J. Org. Chem*. **4** 573; (e) Xing

M M, Xin M, Shen C, Gao J R, Jia J H and Li Y J 2016 Iodine-promoted oxidative coupling reaction: a simple and efficient process to access imidazo[1,2-*a*]pyridines from 2-aminopyridines and chalcones *Tetrahedron* **72** 4201

13. (a) Ackermann L and Kaspar L T 2007 $TiCl_4$-Catalyzed indirect anti-markovnikov hydration of alkynes: application to the synthesis of benzo[b]furans *J. Org. Chem.* **72** 6149; (b) Dhopte K B, Zambare R S, Patwardhan A V and Nemade P R 2016 Role of graphene oxide as a heterogeneous acid catalyst and benign oxidant for synthesis of benzimidazoles and benzothiazoles *RSC Adv.* **6** 8164
14. (a) Navalon S, Dhakshinamoorthy A, Alvaro M and Garcia H 2014 Carbocatalysis by graphene-based materials *Chem. Rev.* **114** 6179; (b) Dreyer D R, Todd A D and Bielawski C W 2014 Harnessing the chemistry of graphene oxide *Chem. Soc. Rev.* **43** 5288; (c) Su C and LohK P 2013 Carbocatalysts: graphene oxide and its derivatives *Acc. Chem. Res.* **46** 2275
15. (a) Hummers W S and Offemann R E 1958 Preparation of graphitic oxide *J. Am. Chem. Soc.* **80** 1339; (b) Nakajima T and Matsuo Y 1994 Formation process and structure of graphite oxide *Carbon* **32** 469
16. Dreyer D R, Jia H P and Bielawski C W 2010 Graphene oxide: a convenient carbocatalyst for facilitating oxidation and hydration reactions *Angew. Chem. Int. Ed*. **49** 6813; (b) Huang H, Huang J, Liu Y M, He H Y, Cao Y and Fan K N 2012 Graphite oxide as an efficient and durable metal-free catalyst for aerobic oxidative coupling of amines to imines *Green Chem.* **14** 930; (c) Dreyer D R, Jia H P, Todd A D, Jeng G and Bielawski C W 2011 Graphite oxide: a selective and highly efficient oxidant of thiols and sulphides *Org. Biomol. Chem.* **9** 7292
17. Szabo T, Tombacz E, Illes E and Dekany I 2006 Enhanced acidity and pH-dependent surface charge characterization of successively oxidized graphite oxides *Carbon* **44** 537
18. (a) Gupta A, Kour D, GuptaV K and Kapoor K K 2016 Graphene oxide mediated solvent-free three component reaction for the synthesis of 1-amidoalkyl-2-naphthols and 1,2-dihydro-1-arylnaphth[1,2-*e*][1,3]oxazin-3-ones *Tetrahedron Lett*. **57** 4869; (b) Shaabani A, Mahyari M and Hajishaabanha F 2014 The synthesis of xanthenes and benzoxanthenes on graphene oxide and sulfated graphene nanosheets in water *Res. Chem. Intermed.* **40** 2799; (c) Chen M, Luo Y, Zhang C, Guo L, Wang Q and Wu Y 2019 Graphene oxide mediated thiolation of indoles in water: a green and sustainable approach to synthesize 3-sulfenylindoles *Org. Chem. Front.* **6** 116; (d) Fang J, Peng Z, Yang Y, Wang J Guo J and Gong H 2018 Graphene-oxide-promoted direct dehydrogenative coupling reaction of aromatics *Asian J. Org. Chem*. **7** 355
19. (a) Kour D, Gupta A, Kapoor K K, Gupta V K, Rajnikant, Singh D and Das P 2018 Iodine–NH_4OAc mediated regioselective synthesis of 2-aroyl-3-arylimidazo[1,2-*a*]pyridines from 1,3-diaryl-prop-2-en-1-ones *Org. Biomol. Chem.* **16** 1330; (b) Kour D, Khajuria R and Kapoor K K 2016 Iodine–ammonium acetate promoted reaction between 2-aminopyridine and aryl methyl ketones: a novel approach towards the synthesis of 2-arylimidazo[1,2-*a*]pyridines *Tetrahedron Lett.* **57** 4464
20. (a) Gupta A, Khajuria R and Kapoor K K 2016 Reaction of 3-(2-nitrophenyl)-1-arylprop-2-en-1-ones with triethylphosphite in microwave revisited: One-pot synthesis of 2-aroylindoles and 2-arylquinoline *Synth. Commun.* **46** 31; (b) Saini Y, Khajuria R, Rana L K, Hundal M S, Gupta V K, Rajnikant and Kapoor K K 2016 Unprecedented reaction of ninhydrin with ethyl cyanoacetate and diethyl malonate on ultrasonic irradiation *Tetrahedron* **72** 257; (c) Khajuria R, Kannaboina P, Kapoor K K, Gupta A Raina G, Jassal A K, Rana L V, Hundal M S and Das P 2015 Divergent synthesisof 4,6-diarylated pyridin-2(1*H*)-ones from chalcones: novel access to 2,4,6-triaryl pyridines *Org. Biomol. Chem.* **13** 5944; (d) Kaur R, Gupta A and Kapoor K K 2017 Alum as an efficient catalyst for the multicomponent synthesis of functionalized piperidines *Res. Chem. Intermed*. **43** 6099
21. Xavier P, Sharma K, Elayaraja K, Vasu K S, Sood A K and Bose S 2014 Reduced graphene oxide induced phase miscibility in polystyrene–poly(vinyl methyl ether) blends *RSC Adv.* **4** 12376
22. Kumar M, Singh R, Khajuria H and Sheikh H N 2017 Facile hydrothermal synthesis of nanocomposites of nitrogen doped graphene with metal molybdates (NG-$MMoO_4$) M=Mn, Co, and Ni) for enhanced photodegradation of methylene blue *J. Mater. Sci: Mater. Electron*. **28** 9423